
Optoelectronic properties of silver doped copper oxide thin films

Vishal Mohade¹, Krishna Kumar¹ Parasuraman Swaminathan^{1,2*}

¹Electronic Materials and Thin Films Lab, Dept. of Metallurgical and Materials Engineering,
Indian Institute of Technology, Madras, Chennai, India

²Centre of Excellence in Ceramics Technologies for Futuristic Mobility,
Indian Institute of Technology Madras, Chennai, India

*Email: swamnthn@iitm.ac.in

Abstract

Thin films have found a wide variety of applications because of the substantial improvement in their properties as compared to bulk metals. Metal oxide thin films are increasingly being used in various fields and are especially important in functional applications. They can be either *p*- or *n*-type in nature depending on the materials, dopants, and preparation route. Copper oxide is an example of a *p*-type metal oxide, which finds application in solar cells, photo-electrochemical cells, gas sensors, supercapacitors, and thermoelectric touch detectors. Both copper (I) and copper (II) oxides can be grown with the lower valence state oxide stable at low temperature and the higher valence state obtained by annealing at higher temperatures. In this work, we modify the optical and electrical properties of copper oxide thin films, by doping of silver through a thermal evaporation process route. Copper is thermally evaporated onto the substrate and silver is co-evaporated during this process. The films are then annealed in ambient under various conditions to obtain copper oxide. Structural and functional comparison is made between undoped and silver doped copper oxide thin films, prepared under the same conditions. Thermal evaporation is a simple route for obtaining doped metal oxides and the process can be extended to a variety of other systems as well.

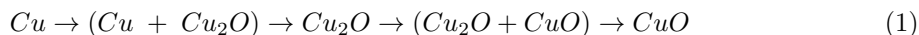
Keywords: Copper oxide; Thermal evaporation; Optoelectronic properties; Electron microscopy; Silver doping

1 Introduction

Copper oxide is a well-studied material because of the abundance of copper in nature, its p -type conductivity, easy synthesis by oxidation of copper, good optical and electrical properties, and non-toxic nature. There are various methods to produce copper oxide thin films viz. thermal evaporation [1–4], magnetron sputtering [5], electrodeposition [6–9], chemical vapor deposition [10], chemical bath deposition [11–13], plasma sputtering [14], molecular beam epitaxy, DC reactive sputtering [15], RF reactive sputtering [16, 17], ion beam sputtering [18], sol-gel [19, 20], and pulsed laser deposition [21].

There have been several studies to determine the properties of copper oxide thin films. Pure copper film on annealing is found to form different oxides at different annealing temperatures. The first oxide is cuprous oxide (Cu_2O), which starts forming in range of 200-250 °C and exhibits and optical bandgap of 2.0-3.0 eV, with cubic crystal structure of lattice parameter 0.427 nm. The higher valence, cupric oxide (CuO) starts forming above 300 °C and has a optical bandgap of 1.2-1.7 eV. CuO shows monoclinic crystal structure and both oxides show p -type conductivity [1, 4, 5]. These oxides shows promising applications in gas sensors [22–24], solar cells [15, 25, 26], thermoelectric touch sensors [2], thin film transistors [3], and supercapacitors [11], to name a few. Thermal evaporation produces very uniform films with no porosity, and high adhesion. It is a non-toxic and line of sight process.

The Cu-Ag phase diagram [27] shows a eutectic obtained at 71.9 wt. % Ag. For temperatures below 400 °C and very low concentration of Ag there is negligible mixing or solubility of Ag in Cu. The pressure vs. temperature diagram for the Cu-O system [28] shows that at a pressure greater than 100 Torr and temperatures higher than 600 °C, copper oxide exists as CuO . Papadimitropoulos *et al.* deposited copper oxide thin films using thermal vacuum evaporator on a silicon substrate [4]. On oxidation, the film showed cuprous oxide formation at 225 °C, copper silicides were also seen at this temperature. At 280 °C, Cu_2O amount starts to decrease and CuO peaks appear, which then converts to only CuO peaks at 350 °C. CuO forms because the Gibbs free energy for the oxidation of Cu_2O to CuO at a temperature of 200 °C is -3.73 kcal/mol [29]. Chaudhary *et al.* justified it as the supply of thermal energy to the cubic Cu_2O should cause higher ionicity and smaller grain size to transform into lower symmetry and larger grain size [30]. Figueredo *et al.* observed similar peaks of Cu_2O (111) from 250 to 300 °C and CuO (11-1) above 300 °C by using e-beam evaporation of pure copper sample on glass slide followed by annealing [2]. Thus, the overall conversion can be written as



In this work we attempted addition of silver nanoparticles on the surface of a copper thin film without breaking vacuum. We used a thermal evaporation process route to ascertain efficient film morphology for study of the functional properties. The as deposited samples were then annealed to obtain oxides. The study of morphology helped us to understand grain development with temperature. A variety of characterization tools were used to study the effects of silver addition. The optical properties showed the bandgap values of copper oxide similar to others. Similar work has been attempted by only one other researcher, who used microwave annealing process to study optical properties of silver doped copper oxide thin film [31]. Li-doped copper oxide thin films also shows a decrease in band gap with Li concentration [?]. The doping process for copper oxide thin film has not been adapted elsewhere. The effect on electrical properties because of doping copper oxide have not yet been reported. This work will give a brief information about changes in resistance and carrier concentration by silver doping. The effect of temperature on resistance of copper oxide thin film can also help to develop a temperature sensor. These properties were studied elsewhere with computational modelling using density functional theory [32].

2 Materials and methods

Copper thin films were deposited on microscopic glass slides using high vacuum coating unit (Model HPVT 303) by Hydro Pneo Vac Technology. Prior to deposition, the glass slides were cut to dimension of $2.5 \times 2.5 \text{ cm}^2$. Then they were cleaned in steps of 1 % soap solution, deionized water, ethanol and deionized water again by ultra-sonication for 15 min in each solution. These were dried by wiping with lint free cloth. The deposition was performed at high vacuum level (7×10^{-6} mbar). The rate of deposition was maintained for all depositions to be 0.14 nm s^{-1} . Thin film thickness was monitored with a quartz crystal microbalance. The substrate was kept at room temperature and no external heating was provided during deposition, though there was a rise in temperature of the substrate during thermal evaporation. Silver thin film of thickness 1 nm were deposited on top of the pure copper film, without breaking vacuum. The deposited thin film was then annealed at temperatures from 150 to 450 °C at an interval of 100 °C. The annealing was performed in a muffle furnace in ambient atmosphere. The heating rate was maintained at 5 °C/min and the holding time was 2 h. Both pure copper and silver doped copper films were annealed under the same conditions.

Grazing incidence x-ray diffraction (GIXRD) measurements were performed on a Rigaku Smartlab XRD machine with 9 kW rotating anode X-ray source. The configuration includes Cu as the source material and Ge monochromator. The incidence angle was maintained at 1 ° and 2θ was varied at the scanning rate of 0.01 ° per s. The analysis was done using XPert Highscore pro. cUV-Visible spectroscopy was performed on a Jasco V-730 spectrophotometer, with halogen and deuterium lamps as sources. The wavelength range for measurement was 200 – 1100 nm. Raman spectroscopy was performed using NdYAG laser of wavelength 532 nm on WiTech alpha 300 confocal Raman microscope. The accumulation time was kept at 5 s. The objective used was 20 ×. For photoluminescence spectroscopy (PL) Jasco FP 6300 was used. The excitation wavelengths used were 320 nm and 450 nm. A DC powered 150 W Xe lamp was used as a source. The accumulation and integration time were set at 10 s respectively. Electrical transport measurement was carried out in Van der Pauw setup on DynaCool PPMS by Quantum design at room temperature. All measurements were done at 300 K. The contacts were made using silver paint adhesive and copper wire. The sample dimensions were maintained at 4 mm × 4mm ($L \times W$). $I - V$ measurements were performed in a four-probe setup on a source meter, Keysight precision measurement system. The contacts were made using silver epoxy adhesive and copper wires. Voltage range was kept as -10 V to 10 V. $I - V$ measurement with temperature (Seebeck coefficient) was done on Cascade Microtech summit 12000 AP. The temperature range was from room temperature to 120 °C in steps of 10 °C and ETC 200L (Espec corp.) thermos chuck was used to monitor temperatures. The voltage range was -10 to 10 V. Sheet resistance was measured on Jandel mode RM 3000 using a four probe configuration. The equipment was calibrated and zeroed before taking readings. The current was automatically set by equipment within range of 10 nA to 99.99 mA. Scanning electron microscopy was done on FEI Quanta 400 high resolution scanning electron microscope. The detector used was Everhart Thornley detector (ETD). Transmission electron microscopy was performed on FEI Tecnai 12 electron microscope.

3 Results and Discussion

3.1 Structural characterization

On annealing of samples, visually, we can clearly deduce that the sample with 250 °C annealing temperature was the most transparent. Annealing at lower temperatures, 150 °C, produced samples which were opaque, while at the highest temperature of 450 °C, the annealed sample was more transparent than 350 °C annealed sample. The optical images are summarized in figure 1 and the samples are kept above IITM logo for showcasing their transparency.

To identify the phases, XRD studies were carried out on copper oxide and silver doped copper

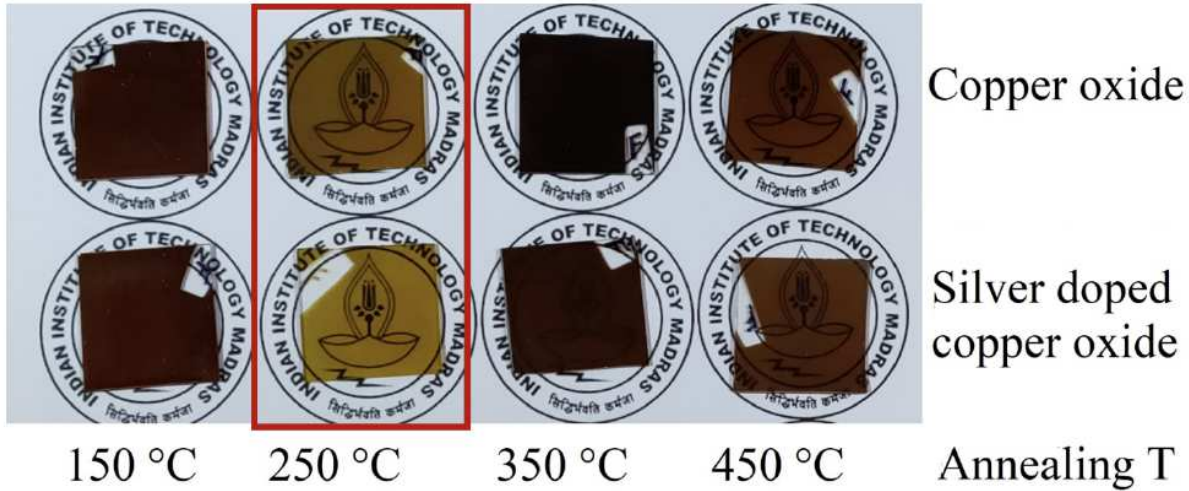


Figure 1. Comparison of optical images of annealed pure copper oxide and silver doped copper oxide thin films.

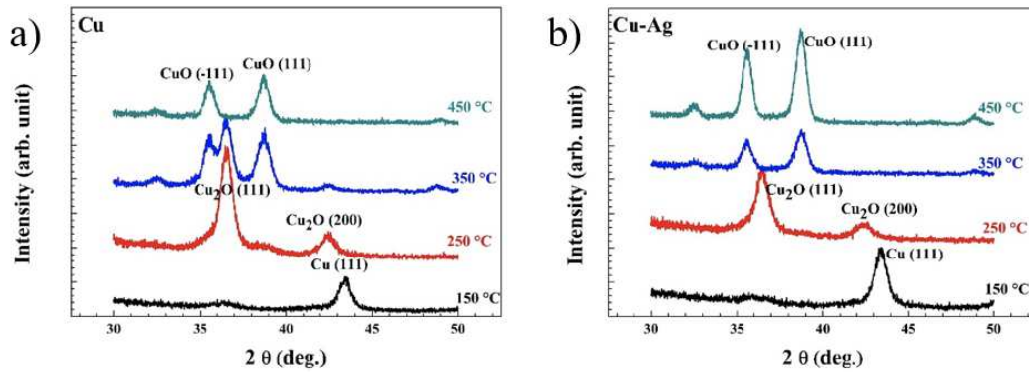
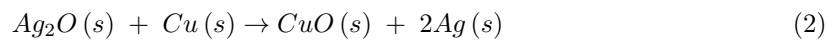


Figure 2. GIXRD of a) undoped copper oxide b) silver doped copper oxide thin film at different annealing temperatures.

oxide thin films. The XRD patterns were measured for thin films annealed at temperatures from 150 to 450 °C. GIXRD results, presented in figure 2 (a) and (b), showed the presence of copper peaks in 150 °C annealed sample (ICDD number: 01-085-1326), indicating incomplete oxidation at this temperature. Samples annealed at 250 °C showed peaks at 36.5 °corresponding to Cu_2O (111) and at 42.2 °corresponding to Cu_2O (200) (ICDD number: 05-667). Samples annealed at 350 °C showed peaks at 35.5 °and 38.7 °corresponding to CuO [ICDD number: 45-0937] and samples annealed at 450 °C showed 35.5 °and 38.7 °peaks. At 150 °C, a copper peak appears at 42.4 °, from Cu (111) plane. The data obtained matches results are obtained by Choudhary *et al.* [1].

The crystallite size variation with temperature and doping can be seen in table 1. The crystallite size was obtained using Hall–Petch equation. For undoped copper oxide thin films the crystallite size decreases with annealing temperature, whereas for Ag doped copper oxide it increases. Ag doping has decreased the crystallite size in films annealed at 150 and 250 °C, when compared to undoped Cu at these temperatures. This is due to higher affinity of copper towards oxygen and the preferential oxidation of copper that occurs in presence of silver [31].



SEM was performed at magnification of $40000 \times$ in secondary electron mode using a Everhart–Thornley detector. Thin films were sputtered with gold before measurement. Typical mi-

Table 1. Variation of crystallite size with temperature.

Annealing temperature (°C)	Crystallite size of undoped copper oxide (nm)	Crystallite size of silver doped copper oxide (nm)
150	33.7	5.2
250	13	6.3
350	8.3	18.8
450	10.6	15.2

crostructure of the thin films, without and with silver, analyzed by SEM are shown figures 3 and 4 respectively. The inset at the bottom left shows the calibration scale to observe the grain size and top right shows the temperature of annealing. Both thin films annealed at 150 °C shows smoother film and very fine grain size and closed packed structure. The grain size increases with annealing temperature. Figure 3 shows undoped copper oxide thin films annealed at different temperatures. The film morphology appears smooth and grain size distribution is uniform. Thin films annealed at 350 °C shows very high increase in grain size as compared to other films. The film annealed at 450 °C shows presence of pores smaller than the grains. Ag doped SEM images, on the other hand, shows smooth and uncracked films. The grains appear well-defined in Ag doped copper oxide thin film (shown in figure 4) and the grain size increases with temperature, which is similar to the undoped copper oxide thin film. The grains agglomerated to form bigger grains, therefore grain size variation in the 450 °C annealed film looks non uniform. A crack is also observed around bigger grains. This crack is due to connecting of adjoining pores. The pore size observed is comparable to the grain size. The 350 °C film shows more layered structure and decreased pore size. On comparing to undoped copper oxide thin film annealed at 450 °C in figure 3, the Ag doped thin film shows aggregated grains with more defined shape of top layer.

To get closer look at the grain structure on the addition of silver to copper thin films, representative TEM images of the as deposited copper and silver doped copper thin films are shown in figure 5. Figure 5 (a) shows a uniform grain size for pure copper, whereas in figure 5 (b) the grain size is non uniform and there are some grains which are distributed randomly with larger size as compared to rest of the grains and the smaller grains shows similar size as in fig 5 (a). By comparison between (a) and (b) we can conclude that the bigger grains are of Ag doped copper.

3.2 Optical properties

Figure 6 shows the absorbance plot for both doped and undoped copper oxide thin films. The absorbance is high in the UV region due to the opaque nature of the thin film. Silver doped thin film shows higher absorbance in blue region as compared to undoped copper oxide. This may be due to the nature of noble metals such as silver. They absorb light due to the transition of electrons between unoccupied hybridized sp states and occupied d states. Absorbance decreases with increase in wavelength till 500 nm (blue green region) for undoped thin film. A similar behavior is shown by silver doped copper oxide annealed at 250 °C. The optical band gap of copper oxide thin films can be calculated using Tauc equation and figure 7 shows the Tauc plot for determining the band gap of CuO and Ag doped CuO thin films. Band gap values can be seen from the extrapolation of the linear portion of to the energy axis of the Tauc plot (arrow pointing on X-axis). Cu₂O has a direct band gap of 2.91 ± 0.3 eV and CuO has indirect band gap of 1.5 ± 0.3 eV. The data obtained is similar to those obtained in literature [1–3]. The band gap of silver doped Cu₂O is 3.04 ± 0.3 eV and CuO is 1.70 ± 0.3 eV.

Figure 8 shows Raman spectra of annealed copper oxide thin films. Among nine optical modes of CuO, three are Raman active ($A_g + 2 B_g$). The peaks 298, 342 and 627 cm^{-1} corresponds to CuO and the peaks 143, 210, and 617 cm^{-1} correspond to Cu₂O. 450 °C Ag doped copper oxide thin film shows all three CuO peaks only. On the other hand, other temperatures show the presence of Cu₂O peaks more dominantly. The silver doped copper oxide thin film annealed at

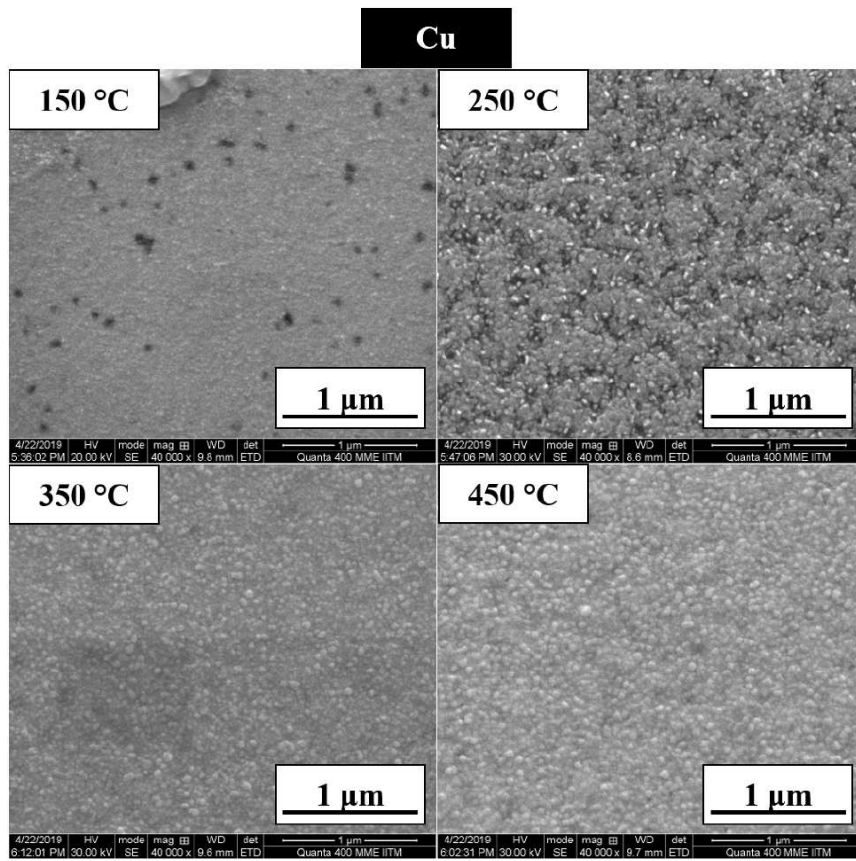


Figure 3. SEM images of pure copper oxide thin film annealed at 150, 250, 350, and 450 °C.

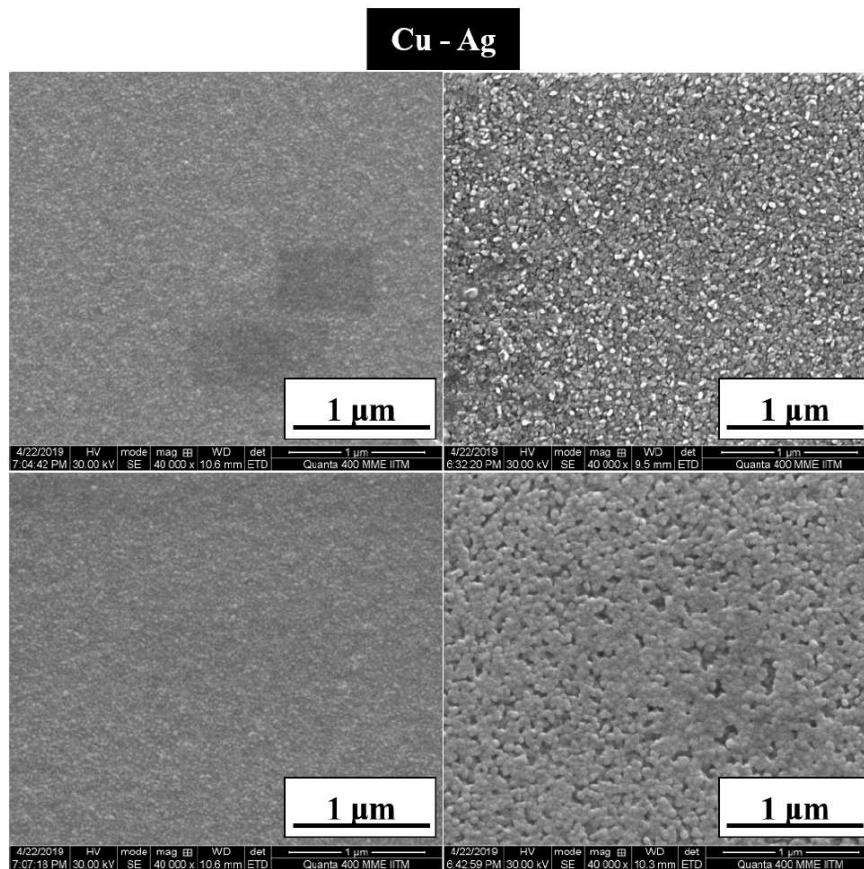


Figure 4. SEM images of Ag doped copper oxide thin film annealed at 150, 250, 350, and 450 °C.

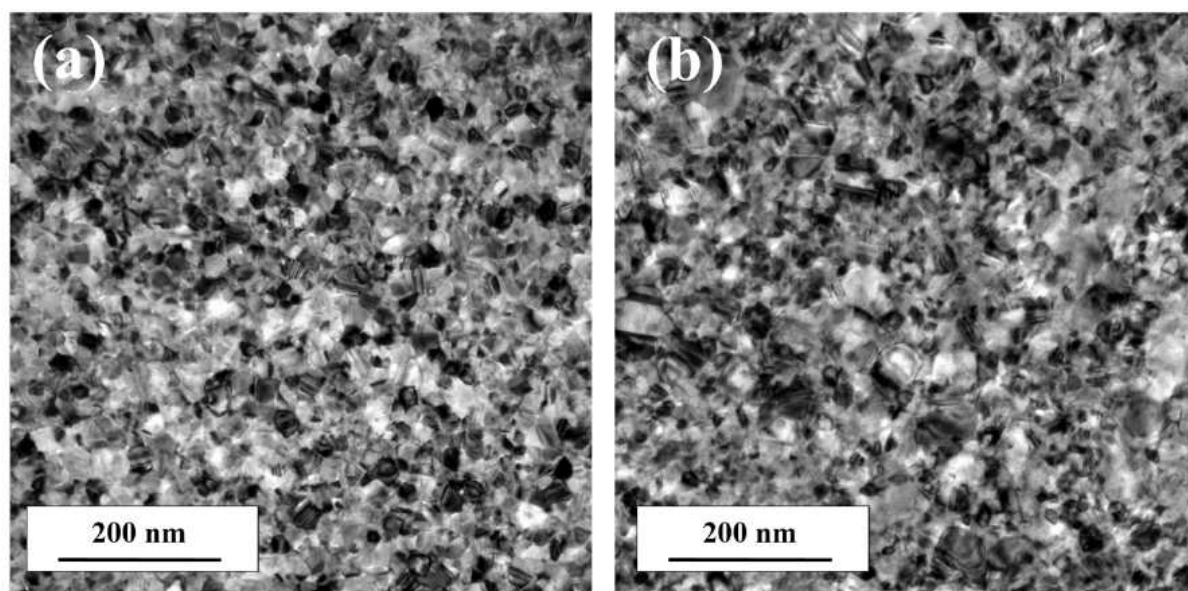


Figure 5. TEM image of a representative sample of a) pure copper and b) silver doped copper

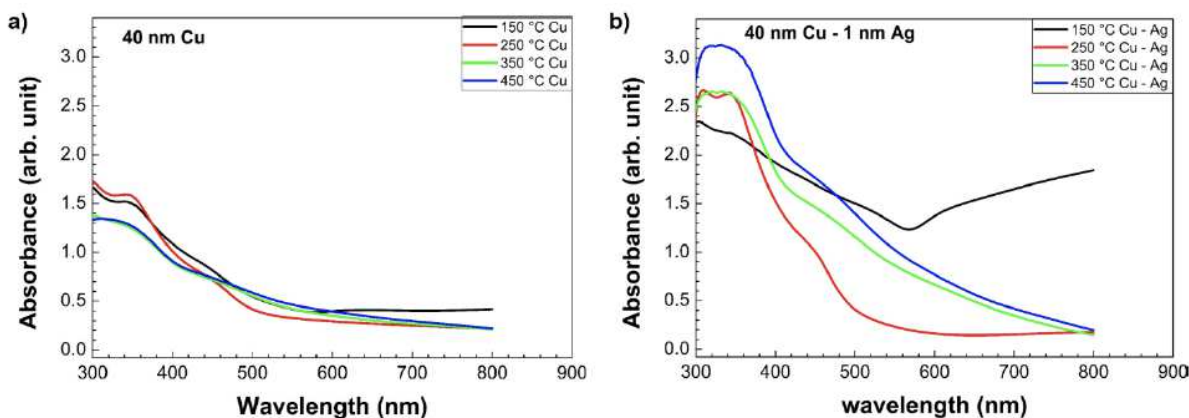


Figure 6. Variation of absorbance with wavelength for a) pure copper oxide thin film and b) silver doped copper oxide thin film.

250 °C shows the greatest intensity of peaks at 143 and 210 cm^{-1} . This can be attributed to the presence of Cu_2O . Raman data confirms the results obtained by XRD. Undoped and doped copper oxide films annealed at 150 °C shows only one peak corresponding to Cu_2O at 1100 cm^{-1} . This signifies the presence of very thin oxide layer, although no other peaks are available. This can suggest that the oxide formation has not started properly at 150 °C.

Photoluminescence spectra were also recorded for the undoped and doped copper oxide thin films. The film annealed at 250 °C shows peaks at 398 nm (near UV emission) and 496 nm (corresponding to cyan emission). The peaks at 540 and 578 nm correspond to green and yellow emissions respectively. The presence of high yellow peaks indicates excess oxygen whereas green emissions indicates oxygen deficiency [33,34]. Both doped and undoped copper oxide thin films annealed at 450 °C exhibit emission in UV range i.e. 364 nm, which can be correlated to band gap transition in CuO [34]. The green emissions are also associated with the presence of surface defects and transition of carriers from near conduction band (oxygen vacancies) to deep valence band (Cu vacancies). Figure 9 shows PL spectra for undoped and doped copper oxide thin films at an excitation wavelength 450 nm. The graph shows a single red emission, this can be due to neutral and single ionized oxygen transitions or deep level emission related to presence of defect [35,36].

3.3 Electrical properties

Electrical transport measurements were performed with Van der Pauw method to obtain carrier concentrations. It shows the resistance value obtained for undoped copper oxide thin films annealed at 250 and 450 °C are 12-20 $\text{M}\Omega$ and 2.8 $\text{M}\Omega$ respectively. For silver doped thin film, annealed at 450 °C, the corresponding value was 22-30 $\text{k}\Omega$. The carrier concentration values for undoped Cu_2O thin film were in range of 10^{15} cm^{-3} and for doped CuO in range of 10^{16} cm^{-3} . The nature of the Hall coefficient shows *p*-type conductivity in copper oxide thin films [2,3,5].

Table 2 shows the sheet resistance values obtained by four probe measurement. The films annealed at 150 °C showed same resistance as copper because of negligible surface oxidation. The resistance is very low for undoped copper oxide thin films as compared to silver doped copper oxide thin films. The increase in resistance is due to increased scattering centers by the addition of silver.

The *I* – *V* curves were also obtained for undoped and silver doped copper oxide thin films. The undoped copper oxide thin film annealed at 450 °C shows non-linear behavior, while the other samples showed Ohmic behavior. The resistance values obtained were similar to those obtained by four-probe data. The temperature dependence of resistance was also measured and the values are listed in table 3. The table shows that the resistance decreases with increase in temperature

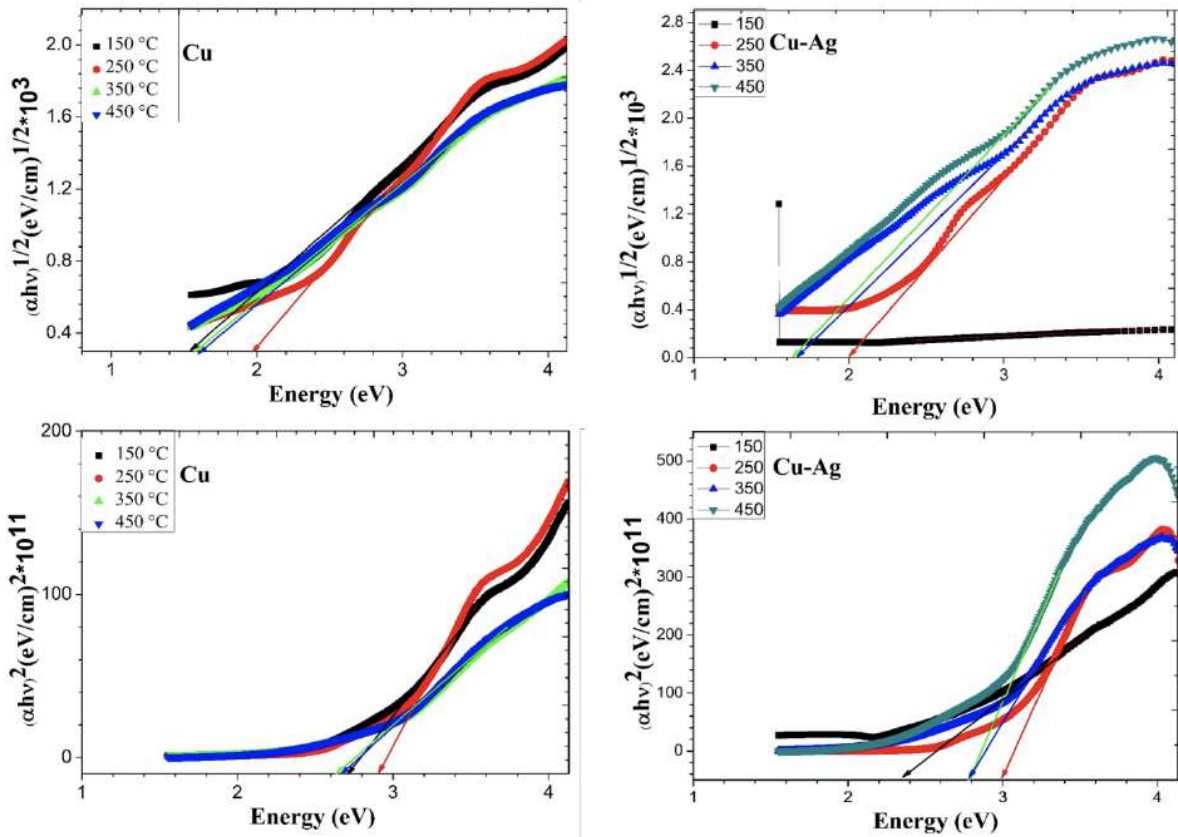


Figure 7. Tauc plot for undoped and Ag doped Copper oxide thin films.

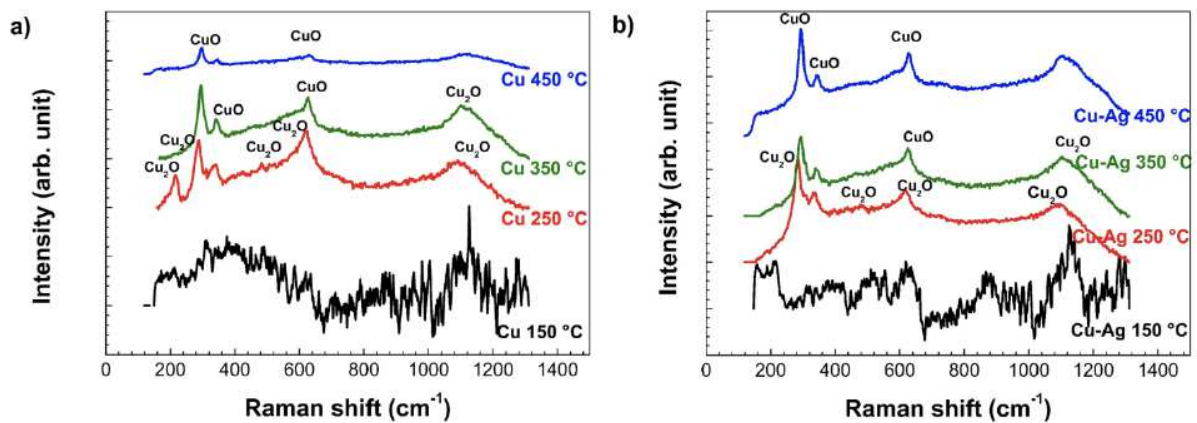


Figure 8. Raman spectra of annealed a) undoped copper oxide and b) silver doped copper oxide thin films.

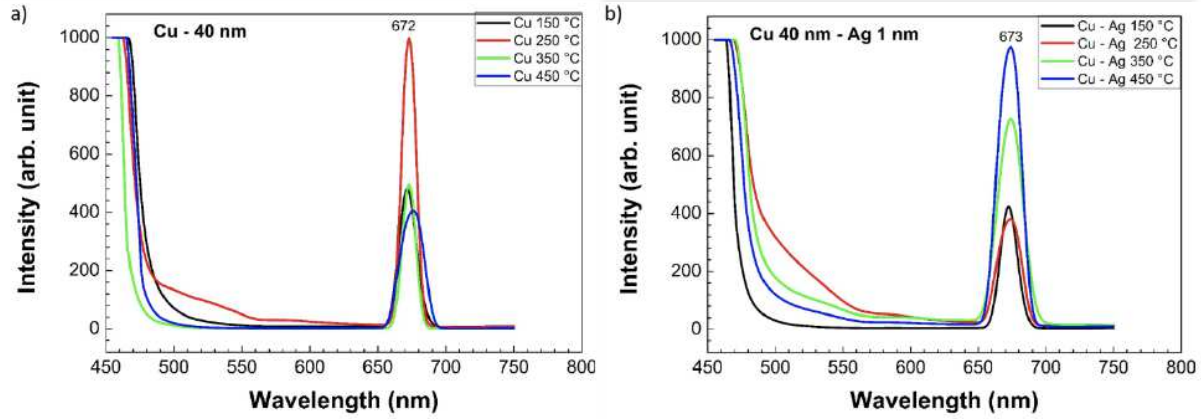


Figure 9. Photoluminescence (PL) spectra of a) undoped copper oxide thin film and b) silver doped copper oxide thin film with an excitation wavelength 450 nm.

Table 2. Sheet resistance values obtained by four probe measurement.

Annealing temperature (°C)	Undoped copper oxide ($\Omega/sq.$)	Silver doped copper oxide ($\Omega/sq.$)
150	1.2	1.1
250	4×10^6	66×10^6
350	10×10^6	24.7×10^6
450	1.3×10^6	19×10^6

for all the annealed thin films. The drop in the resistance for silver doped thin film annealed at 250 °C is very drastic, but the initial resistance value is very high which also can be seen from the table. This decrease is not regular for undoped copper oxide thin film annealed at 250 °C. The decrease for silver doped thin film annealed at 450 °C is gradual with temperature, which makes it a great choice for temperature sensor application.

Table 3. Resistance variation with temperature for select annealed copper oxide thin films.

Temperature (°C)	Resistance of Cu 250 °C (M Ω)	Resistance of Cu-Ag 250 °C (M Ω)	Resistance of Cu-Ag 450 °C (M Ω)
22	33.3	203	14.7
50	9.05	92.7	9.37
60	17.9	69	8.02
70	6.66	52.3	6.71
80	8.87	42.1	6.1
90	5.95	30.5	5.49
100	6.34	23.1	4.61

4 Conclusion

Copper oxide thin film annealed at 250 °C shows the highest optical transparency. XRD studies show the presence of Cu_2O phase in both undoped and silver doped copper oxide thin films annealed at 250 °C. CuO phase starts forming above 330 °C and hence it is visible in XRD pattern of thin films annealed at 350 and 450 °C. Raman spectroscopy also confirms the results obtained

by XRD. On increasing the annealing temperature, the grain size increased. Silver doped copper oxide thin films showed larger band gap than undoped copper oxide thin films. The blue and green emission showed deficiency or excess of oxygen in thin films, and red emission showed transition of single and ionized oxygen. Copper oxide thin films showed *p*-type conductivity. Silver doped copper oxide thin films showed higher resistance than undoped copper oxide. The resistance value decreases with increase in temperature for all copper oxide thin films. The resistance variation of silver doped copper oxide thin film annealed at 450 °C with temperature showed a possible application as temperature sensor.

Acknowledgments

Support from the Centre of Excellence in Ceramics Technologies for Futuristic Mobility (project number SB22231272MMETWO008702) is acknowledged. Electron microscopy (SEM and TEM) was carried out at the facilities available in the Dept. of Metallurgical and Materials Engineering, IIT Madras. Optical characterisation was performed at the facilities available at the Dept. of Physics, IIT Madras, while electrical characterisation was carried out at the Centre for NEMS and Nanophotonics, IIT Madras.

References

1. Sumita Choudhary, JVN Sarma, and Subhashis Gangopadhyay. Growth and characterization of single phase cu₂o by thermal oxidation of thin copper films. In *AIP Conference Proceedings*, volume 1724, page 020116. AIP Publishing LLC, 2016.
2. Joana Figueira, Joana Loureiro, Jose Marques, Catarina Bianchi, Paulo Duarte, Mikko Ruoho, Ilkka Tittonen, and Isabel Ferreira. Optimization of cuprous oxides thin films to be used as thermoelectric touch detectors. *ACS Applied Materials & Interfaces*, 9(7):6520–6529, 2017.
3. V Figueiredo, JV Pinto, J Deuermeier, R Barros, E Alves, R Martins, and E Fortunato. *p*-type thin-film transistors produced by thermal oxidation. *Journal of Display Technology*, 9(9):735–740, 2013.
4. G Papadimitropoulos, N Vourdas, V Em Vamvakas, and D Davazoglou. Deposition and characterization of copper oxide thin films. In *journal of physics: conference series*, volume 10, page 045. IOP Publishing, 2005.
5. Dhanya S Murali, Shailendra Kumar, RJ Choudhary, Avinash D Wadikar, Mahaveer K Jain, and A Subrahmanyam. Synthesis of cu₂o from cuo thin films: Optical and electrical properties. *AIP advances*, 5(4):047143, 2015.
6. V Dhanasekaran, T Mahalingam, R Chandramohan, Jin-Koo Rhee, and JP Chu. Electrochemical deposition and characterization of cupric oxide thin films. *Thin Solid Films*, 520(21):6608–6613, 2012.
7. X Mathew, NR Mathews, and PJ Sebastian. Temperature dependence of the optical transitions in electrodeposited cu₂o thin films. *Solar energy materials and solar cells*, 70(3):277–286, 2001.
8. O Messaoudi, M Gannouni, A Souissi, H Makhlof, A Bardaoui, R Chtourou, et al. Structural, morphological and electrical characteristics of electrodeposited cu₂o: effect of deposition time. *Applied Surface Science*, 366:383–388, 2016.

-
9. Adriana Paracchino, Vincent Laporte, Kevin Sivula, Michael Grätzel, and Elijah Thimsen. Highly active oxide photocathode for photoelectrochemical water reduction. *Nature materials*, 10(6):456–461, 2011.
 10. Davide Barreca, Alberto Gasparotto, and Eugenio Tondello. Cvd cu₂o and cuo nanosystems characterized by xps. *Surface Science Spectra*, 14(1):41–51, 2007.
 11. DP Dubal, DS Dhawale, RR Salunkhe, VS Jamdade, and CD Lokhande. Fabrication of copper oxide multilayer nanosheets for supercapacitor application. *Journal of Alloys and Compounds*, 492(1-2):26–30, 2010.
 12. Zheng-Dong Lin, Shoou-Jinn Chang, Yi-Hao Chen, and Ting-Jen Hsueh. Copper oxide thin films prepared by chemical bath deposition technique. In *2015 IEEE 42nd Photovoltaic Specialist Conference (PVSC)*, pages 1–3. IEEE, 2015.
 13. Jenifar Sultana, Somdatta Paul, Anupam Karmakar, Ren Yi, Goutam Kumar Dalapati, and Sanatan Chattopadhyay. Chemical bath deposited (cbd) cuo thin films on n-silicon substrate for electronic and optical applications: impact of growth time. *Applied surface science*, 418:380–387, 2017.
 14. Zhenzhen Li, Kemeng Tong, Ruifang Shi, Yonglong Shen, Yiqiang Zhang, Zhiqiang Yao, Jiajie Fan, Mike Thwaites, and Guosheng Shao. Reactive plasma deposition of high quality single phase cuo thin films suitable for metal oxide solar cells. *Journal of Alloys and Compounds*, 695:3116–3123, 2017.
 15. Yahya Alajlani, Frank Placido, Hin On Chu, Robert De Bold, Lewis Fleming, and Des Gibson. Characterisation of cu₂o/cuo thin films produced by plasma-assisted dc sputtering for solar cell application. *Thin Solid Films*, 642:45–50, 2017.
 16. S Ghosh, DK Avasthi, P Shah, V Ganesan, A Gupta, D Sarangi, R Bhattacharya, and W Assmann. Deposition of thin films of different oxides of copper by rf reactive sputtering and their characterization. *Vacuum*, 57(4):377–385, 2000.
 17. D Hartung, F Gather, P Hering, C Kandzia, D Reppin, A Polity, BK Meyer, and PJ Klar. Assessing the thermoelectric properties of cu x o (x= 1 to 2) thin films as a function of composition. *Applied Physics Letters*, 106(25):253901, 2015.
 18. P Horak, V Bejsovec, J Vacik, V Lavrentiev, M Vrnata, M Kormunda, and S Danis. Thin copper oxide films prepared by ion beam sputtering with subsequent thermal oxidation: application in chemiresistors. *Applied Surface Science*, 389:751–759, 2016.
 19. NA Raship, MZ Sahdan, F Adriyanto, MF Nurfazliana, and AS Bakri. Effect of annealing temperature on the properties of copper oxide films prepared by dip coating technique. In *AIP Conference Proceedings*, volume 1788, page 030121. AIP Publishing LLC, 2017.
 20. Sekhar C Ray. Preparation of copper oxide thin film by the sol–gel-like dip technique and study of their structural and optical properties. *Solar energy materials and solar cells*, 68(3-4):307–312, 2001.
 21. Prakash Chand, Anurag Gaur, Ashavani Kumar, and Umesh Kumar Gaur. Structural and optical study of li doped cuo thin films on si (1 0 0) substrate deposited by pulsed laser deposition. *Applied surface science*, 307:280–286, 2014.
 22. Kevin Limkrailassiri. *Copper oxide by thermal oxidation for electrochemical cells and gas sensors*. PhD thesis, UC Berkeley, 2013.

-
23. Nafarizal Nayan, Mohd Zainizan Sahdan, Low Jia Wei, Mohd Khairul Ahmad, Jais Lias, Soon Chin Phong, Ali Yeon Md Shakaff, Ammar Zakaria, and Ahmad Faizal Mohd Zain. Correlation between microstructure of copper oxide thin films and its gas sensing performance at room temperature. *Procedia Chemistry*, 20:45–51, 2016.
 24. YH Navale, ST Navale, FJ Stadler, NS Ramgir, AK Debnath, SC Gadkari, SK Gupta, DK Aswal, and VB Patil. Thermally evaporated copper oxide films: A view of annealing effect on physical and gas sensing properties. *Ceramics International*, 43(9):7057–7064, 2017.
 25. Arne Roos, Teddy Chibuye, and Björn Karlsson. Properties of oxidized copper surfaces for solar applications i. *Solar Energy Materials*, 7(4):453–465, 1983.
 26. Othmane Daoudi, Youssef Qachaou, Abderrahim Raidou, Khalid Nouneh, Mohammed Lharch, and Mounir Fahoume. Study of the physical properties of cuo thin films grown by modified silar method for solar cells applications. *Superlattices and microstructures*, 127:93–99, 2019.
 27. A Kawecki, T Knych, E Sieja-Smaga, A Mamala, P Kwaśniewski, G Kiesiewicz, B Smyrak, and A Pacewicz. Fabrication, properties and microstructures of high strength and high conductivity copper-silver wires. *Archives of Metallurgy and Materials*, 57:1261–1270, 2012.
 28. L Schramm, G Behr, W Löser, and K Wetzig. Thermodynamic reassessment of the cu-o phase diagram. *Journal of Phase Equilibria and Diffusion*, 26:605–612, 2005.
 29. AO Musa, T Akomolafe, and MJ Carter. Production of cuprous oxide, a solar cell material, by thermal oxidation and a study of its physical and electrical properties. *Solar Energy Materials and Solar Cells*, 51(3-4):305–316, 1998.
 30. Sumita Choudhary, JVN Sarma, Surojit Pande, Soraya Ababou-Girard, Pascal Turban, Bruno Lepine, and Subhashis Gangopadhyay. Oxidation mechanism of thin cu films: A gateway towards the formation of single oxide phase. *AIP Advances*, 8(5):055114, 2018.
 31. Sayantan Das and TL Alford. Structural and optical properties of ag-doped copper oxide thin films on polyethylene naphthalate substrate prepared by low temperature microwave annealing. *Journal of applied physics*, 113(24):244905, 2013.
 32. H Absike, M Hajji, H Labrim, A Abbassi, and H Ez-Zahraouy. Electronic, electrical and optical properties of ag doped cuo through modified becke-johnson exchange potential. *Superlattices and Microstructures*, 127:128–138, 2019.
 33. Anirban Mitra, RK Thareja, V Ganesan, A Gupta, PK Sahoo, and VN Kulkarni. Synthesis and characterization of zno thin films for uv laser. *Applied Surface Science*, 174(3-4):232–239, 2001.
 34. AB Djurišić, YH Leung, KH Tam, L Ding, WK Ge, HY Chen, and S Gwo. Green, yellow, and orange defect emission from zno nanostructures: Influence of excitation wavelength. *Applied Physics Letters*, 88(10), 2006.
 35. A El Hichou, M Addou, J Ebothé, and M Troyon. Influence of deposition temperature (ts), air flow rate (f) and precursors on cathodoluminescence properties of zno thin films prepared by spray pyrolysis. *Journal of luminescence*, 113(3-4):183–190, 2005.
 36. K Vanheusden, CH Seager, WL t Warren, DR Tallant, and JA Voigt. Correlation between photoluminescence and oxygen vacancies in zno phosphors. *Applied physics letters*, 68(3):403–405, 1996.